February 23, 2005

A macroscopic chemistry method for the direct simulation of gas flows

Charles R. Lilley and Michael N. Macrossan

Centre for Hypersonics, The University of Queensland, St. Lucia, 4072, Australia

(Final manuscript, published in: *Physics of Fluids* **16**(6), June 2004, pp. 2054–2066)

Abstract

In most chemistry methods developed for the direct simulation Monte Carlo (DSMC) technique, chemical reactions are computed as an integral part of the collision simulation routine. In the macroscopic chemistry method developed here, the simulation of collisions and reactions are decoupled in that reactions are computed independently, after the collision routine. The number of reaction events to perform in each cell is calculated using the macroscopic reaction rates $k^{\pm}$ and equilibrium constant K^*, with local macroscopic flow conditions. The macroscopic method is developed for the symmetrical diatomic dissociating gas. For each dissociation event, a single diatomic simulator particle is selected with a probability based on its internal energy, and is replaced by two atomic particles. For each recombination event, two atomic particles are selected at random, and are replaced by a single diatomic particle. The dissociation energy is accounted for by adjusting the translational thermal energies of *all* particles in the cell. The macroscopic method gives density profiles in agreement with experimental data for the chemical relaxation region downstream of a strong shock in nitrogen. In the non-equilibrium regions within the shock, and along the stagnation streamline of a blunt cylinder in rarefied flow, the macroscopic method gives results in excellent agreement with those obtained using the most common conventional DSMC chemistry method in which reactions are calculated during the collision routine. The number of particles per computational cell has a minimal effect on the results provided by the macroscopic method. Unlike most DSMC chemistry methods, the macroscopic method is not limited to simple forms of $k^{\pm}$ and K^*. *Any* forms may be used, and these may be *any* function of the macroscopic conditions. This is demonstrated by using a two-temperature rate model, and a form of K^* with a number density dependence. With the two-temperature model, the macroscopic method gives densities in the post-shock chemical relaxation region that also agree with the experimental data. For a form of K^* with a number density dependence, the macroscopic method can accurately reproduce chemical recombination behavior. In a primarily dissociative flow, the number density dependence of K^* has very little effect on the flow. The macroscopic method requires slightly less computing time than the most common DSMC chemistry method.

I. INTRODUCTION

The direct simulation Monte Carlo (DSMC) method, described in detail by Bird,[1] is the most common computational technique for modeling rarefied gas flows of engineering interest. The DSMC method simulates macroscopic gas behavior by considering the motions and collisions of a set of simulator particles, representative of the real gas molecules, within a spatial array of computational cells. The fundamental DSMC simplification is that the simulation of molecular motions and intermolecular collisions are decoupled, in that they are performed independently after a decoupling interval that is small compared to the mean collision time.

In high enthalpy flows, intermolecular collisions can be sufficiently energetic to cause chemical reactions. In general, the probability of a chemical reaction occurring between colliding reactant molecules is a function of the relative translational energy, internal states and relative orientation of the colliding molecules. In most DSMC simulations of reacting flow, the reaction probability P_R is calculated at each collision between reactants where the total collision energy exceeds some threshold criterion. When P_R exceeds a random fraction R_f, which is uniformly distributed in the range [0,1], the reactant species are changed to product species. The energy modes of the product particles are sampled from appropriate energy distributions. The modeling of chemical reactions is therefore an integral part of the collision routine. Here, such procedures will be termed conventional DSMC chemistry methods.

The formulation of an accurate function for P_R depends on a detailed knowledge of the real state-dependent reaction cross-sections. For the diatomic species typically of interest in hypersonic aerodynamics, knowledge of these cross-sections is very limited.[2,3] Consequently, conventional DSMC chemistry methods usually rely on an expression for P_R that reproduces a suitable macroscopic rate equation in the equilibrium limit. The form of P_R is selected to plausibly approximate the real gas behavior, within the limitations of mathematical tractability and numerical stability. Several conventional DSMC chemistry methods have been devised, and a recent summary is given by Boyd.[4] As shown by Boyd *et al.*,[5] P_R calculated using some conventional DSMC chemistry methods can differ significantly from P_R calculated using more accurate quasi-classical trajectory calculations.

Boyd *et al.*[6] used a chemistry method that excluded trace species from the DSMC simulations, and modeled each trace species concentration by solving a macroscopic diffusion equation with a chemical source term. These separate calculations used local flow conditions, obtained from the DSMC simulation of the dominant chemical species. This method of simulating the chemistry of trace species is an example of a decoupled chemistry method, where chemical reactions are performed as a separate step in the DSMC simulation, independent of the collision routine.

Bartel *et al.*[7] and Bartel[8] considered a more general decoupled chemistry scheme for simulating the reactions of all species in a DSMC computation. The method was applied to simulate reactions in a five species chlorine plasma system, where trace species dominate the system behavior of interest. First, the number of reaction events that should take place in a cell during a time step was calculated, based on the local macroscopic flow conditions and macroscopic reaction rates. A chemistry routine was then invoked after the collision routine to perform the required number of reac-

tions. For each reaction event, participating reactant particles were selected from those within the cell. In Ref. 8, participating particles were selected with either equal probabilities, or according to a method analogous to the no time-counter (NTC) technique[9] for selecting collision partners. In this decoupled method, reactions were performed between reactant particles only when the total energy of the selected reactant particles exceeded a reaction energy threshold. It appears that this decoupled method attempts to correctly model the reacting gas behavior at a microscopic level.

In this paper, a simplified decoupled chemistry method is developed for the symmetrical diatomic dissociating gas, and applied to nitrogen. The number of reaction events required in a cell is calculated as for the decoupled method of Refs. 7 and 8. However, in contrast to the method of Ref. 8, no attempt is made to select collision partners when simulating reaction events. For each dissociation event, a *single* diatomic particle is selected from the cell, and is replaced by two atomic particles; the single diatomic particle is selected with a probability based on its internal energy $\epsilon_{\rm int} = \epsilon_{\rm rot} + \epsilon_{\rm vib}$. For each recombination event, two atomic particles are selected at random from the cell, and combined into a single diatomic particle. The dissociation energy is accounted for by adjusting the thermal velocities of *all* particles in the cell. The method considers net reactions only, so no chemistry is performed where chemical equilibrium exists. Clearly, this approach is phenomenological in nature; it does not attempt to model the detailed physics of the reaction processes. Here, this method is called the macroscopic method. The flexibility of the macroscopic method is demonstrated by using different forms of the reaction rate equations, and a number density dependent form of the equilibrium constant which cannot be modeled using current conventional DSMC chemistry methods.

II. THE VARIABLE HARD SPHERE MODEL

This study uses the variable hard sphere (VHS) molecular model, which has a variable total collision cross-section with hard sphere scattering. This combination was first used in the DSMC method by Borgnakke and Larsen,[10] and later by Erofeev and Perepukhov[11] and Bird.[12] The total collision cross-section for a collision between VHS molecules of species A and B is

$$\sigma = \sigma_r \left(g_r/g\right)^{2\upsilon}, \tag{1}$$

where g is the relative speed and σ_r, g_r and υ are VHS constants characteristic of the A + B collision. Here, the reference speed g_r is defined by

$$g_r \equiv (2kT_r/\tilde{m})^{\frac{1}{2}}, \tag{2}$$

where $\tilde{m} \equiv m_{\rm A} m_{\rm B}/(m_{\rm A} + m_{\rm B})$ is the reduced mass of collision partners A and B and T_r is a reference temperature.

From the Chapman-Enskog viscosity theory,[13] Hirschfelder *et al.* [Eq. (8.2-20), p. 529][14] define a quantity

$$\mu_{\rm AB} \equiv \frac{5}{16} \frac{[\pi(2\tilde{m})kT]^{\frac{1}{2}}}{\pi \bar{\Omega}^{(2,2)}_{\rm AB}(T)}, \tag{3}$$

where $\bar{\Omega}^{(2,2)}_{\rm AB}(T)$ is a mean collision cross-section for collisions between molecules of species A and B. The quantity $\mu_{\rm AB}$ may be regarded as the viscosity of a hypothetical gas in which all molecules have mass $2\tilde{m}$ and interact according to an intermolecular potential curve characteristic of A + B collisions.[14] For VHS molecules, it can be shown that

$$\pi\bar{\Omega}^{(2,2)}_{\rm AB}(T) = \sigma_r \frac{\Gamma(4-\upsilon)}{6}\left(\frac{T_r}{T}\right)^{\upsilon},$$

where

$$\sigma_r = \frac{15\pi^{\frac{1}{2}}}{8}\frac{g_r\tilde{m}}{\mu_r\Gamma(4-\upsilon)} \tag{4}$$

is the VHS reference cross-section and $\mu_r = \mu_{\rm AB}(T_r)$ is the reference viscosity at the reference temperature T_r. From Eqs. (2) to (4), $\mu_{\rm AB} = \mu_r(T/T_r)^{\frac{1}{2}+\upsilon}$. The reference temperature T_r, reference viscosity μ_r and υ for each collision pair are obtained from viscosity data $\mu_{\rm AB} = \mu(T)$, and should be selected to match the real viscosity of the gas being simulated over the temperature range of interest.

III. THE MACROSCOPIC CHEMISTRY METHOD

The macroscopic chemistry method is developed here for the symmetrical diatomic dissociating gas, in which the two reactions

$$\begin{array}{lrcl} \text{Reaction 1:} & \mathrm{A_2 + A} & \rightleftharpoons & \mathrm{A + A + A} \quad \text{and} \\ \text{Reaction 2:} & \mathrm{A_2 + A_2} & \rightleftharpoons & \mathrm{A + A + A_2} \end{array} \tag{5}$$

occur. These reactions have forward rate constants k_1^+ and k_2^+ and reverse rate constants k_1^- and k_2^- respectively. The equilibrium constant K^* is

$$K^* = k_1^+/k_1^- = k_2^+/k_2^-.$$

The dissociation fraction α is the mass fraction of the atomic species, given by

$$\alpha \equiv x_{\rm A}/(x_{\rm A} + 2x_{\rm A_2}),$$

where x_i denotes the mole fraction of species i.

In the macroscopic chemistry method, the number of reaction events required in a cell during a simulation time step Δt is calculated from the macroscopic reaction rate. For the symmetrical diatomic gas, the rate of change of α is given by[15]

$$\dot{\alpha} = \left(k_1^+\alpha + k_2^+\frac{1-\alpha}{2}\right)\frac{\rho}{\mathcal{M}_{\rm A}}\left(1-\alpha-\frac{2\rho}{\mathcal{M}_{\rm A}K^*}\alpha^2\right). \tag{6}$$

Here, $\mathcal{M}_{\rm A}$ is the molar mass of the atomic species in kg/kmol. In a cell containing $N_{\rm A}$ and $N_{\rm A_2}$ particles of A and $\rm A_2$ respectively, the change in $N_{\rm A_2}$ during time Δt, denoted $\Delta N_{\rm A_2}$, can be estimated using

$$\Delta N_{\rm A_2} = (N_{\rm A}/2 + N_{\rm A_2})(\alpha - \alpha'). \tag{7}$$

Here, α and α' are the dissociation fractions at times t and $t + \Delta t$ respectively. The macroscopic method simulates the net number of reaction events only; for net dissociation $\Delta N_{\rm A_2} < 0$, for net recombination $\Delta N_{\rm A_2} > 0$ and where chemical equilibrium

exists, no reaction events will be computed. Where the time scale of reactions $1/\dot{\alpha}$ is much greater than the typical collision interval and hence the decoupling step Δt, a simple Euler method can be used to estimate α', giving

$$\Delta N_{\mathrm{A}_2} \approx -(N_{\mathrm{A}}/2 + N_{\mathrm{A}_2})\dot{\alpha}\Delta t. \tag{8}$$

In the case of net dissociation, for each dissociation event, a *single* diatomic particle is selected from those within the cell, with a probability based on the internal energy. Diatomic particles are selected randomly, and are accepted for dissociation if

$$\epsilon_{\mathrm{int}} / \left(\epsilon_{\mathrm{int}}\right)_{\mathrm{max}} > R_f,$$

where $\left(\epsilon_{\mathrm{int}}\right)_{\mathrm{max}}$ is the maximum instantaneous internal energy in the cell. This selection method is adopted to approximate the physics of the dissociation process, because diatomic particles with high internal energies are more likely to dissociate.

It is assumed that all internal energy in the dissociating diatomic particle is manifested as relative translational energy ϵ_g of the two atomic particles after the dissociation event. The center-of-mass velocity $\mathbf{v}_m$ of the new atomic particles equals that of the original diatomic particle, and the direction of $\mathbf{g}$ is random. The change in chemical potential energy ΔE_{cp} is

$$\Delta E_{\mathrm{cp}} = -\Delta N_{\mathrm{A}_2}\epsilon_a, \tag{9}$$

where ϵ_a is the dissociation energy per event. To enforce energy conservation, this change in chemical potential energy is obtained from the translational component of the thermal energy of *all* particles in the cell, as discussed below.

For net recombination, two atomic particles are selected from the cell for each recombination event. The selection of recombining atoms is random and independent of energy. It is assumed that the relative translational energy ϵ_g of the two atomic particles is manifested as the internal energy ϵ_{int} of the new diatomic particle. The vibrational energy level is set to that closest to $\epsilon_{\mathrm{int}}/2$ such that $\epsilon_{\mathrm{vib}} \leq \epsilon_{\mathrm{int}}$, and the rotational energy is $\epsilon_{\mathrm{rot}} = \epsilon_g - \epsilon_{\mathrm{vib}}$. The velocity of the new diatomic particle equals $\mathbf{v}_m$ of the original atomic particles. The change in chemical potential energy ΔE_{cp} is again given by Eq. (9).

To account for the change in chemical potential energy ΔE_{cp} caused by net dissociation or net recombination, the thermal velocities of *all* the N_p particles within the cell are multiplied by a factor Ψ, such that the adjusted i velocity component of particle p is

$$v'_{i,p} = \Psi(v_{i,p} - \bar{v}_i) + \bar{v}_i. \tag{10}$$

Here, $\bar{v}_i$ is the instantaneous mean i velocity of all particles in the cell. The factor Ψ is given by

$$\Psi = \left(1 - \frac{\Delta E_{\mathrm{cp}}}{\sum_{p=1}^{N_p} \epsilon_{\mathrm{tr},p}}\right)^{\frac{1}{2}}. \tag{11}$$

For net dissociation $\Psi < 1$, and for net recombination $\Psi > 1$. Here, $\epsilon_{\mathrm{tr},p}$ is the translational thermal energy of particle p before the reaction events, given by

$$\epsilon_{\mathrm{tr},p} = \epsilon_{x,p} + \epsilon_{y,p} + \epsilon_{z,p}.$$

The translational thermal energy of velocity component i for particle p is

$$\epsilon_{i,p} = m_p \left[(v_p)_i - \bar{v}_i\right]^2 /2.$$

More elaborate energy redistribution schemes may be envisaged, where internal energies could be adjusted in addition to the translational thermal energies. However, there appears to be minimal benefit in adopting such schemes given the apparent accuracy of the current approximate method.

In a very small number of dissociation cases, the amount of translational thermal energy available in a cell may be smaller than $\Delta E_{\rm cp}$. In such cases, the thermal velocities of all particles in the cell are set to zero using $\Psi = 0$, and the excess translational thermal energy in the cell is stored. This excess energy is then removed from the thermal velocities of the particles in the cell at the next time step, by adjusting the velocities according to Eqs. (10) and (11).

The macroscopic chemistry method considers *net* changes in composition only. At equilibrium, there is no net change in composition, so for the macroscopic chemistry method, detailed balance is not an issue. In this respect, the macroscopic method is similar to continuum flow solvers.

A. Calculating the number of reaction events required

From Eqs. (6) and (7), the number of reaction events required in each cell at each time step depends on local values of ρ, α, α', $N_{\rm A}$, $N_{\rm A_2}$, the forward reaction rates k^+, and the equilibrium constant K^*. Usually, k^+ and K^* are functions of the equilibrium temperature T. Under non-equilibrium conditions, T may be replaced by an appropriate kinetic temperature T_k, which could be, for example, the overall kinetic temperature $T_{\rm kin}$ as given in the Appendix.

The quantities ρ, α, α', $N_{\rm A}$, $N_{\rm A_2}$ and T_k are calculated using flowfield samples. Here, time-weighted rather than instantaneous averages have been used, because the required mean number of reaction events, given by

$$\Delta N_{\rm A_2} = \Delta N_{\rm A_2} \left(\langle\rho\rangle, \langle\alpha\rangle, \langle\alpha'\rangle, \langle N_{\rm A}\rangle, \langle N_{\rm A_2}\rangle, \langle T_k\rangle\right)$$

differs from the mean instantaneous value of

$$\langle\Delta N_{\rm A_2} \left(\rho, \alpha, \alpha', N_{\rm A}, N_{\rm A_2}, T_k\right)\rangle.$$

Also, using time-weighted rather than instantaneous samples is more computationally efficient, because flowfield conditions must be calculated less often. The time-weighted averages are obtained from several flowfield samples, where the sampling interval is set to a time greater than that required for the flow to traverse a typical cell width.

In each computational cell, a cumulative total of $\Delta N_{\rm A_2}$ is maintained, denoted $\sum \Delta N_{\rm A_2}$. At every time step, this cumulative total is updated according to $\Delta N_{\rm A_2}$ calculated from Eq. (7), using stored time-weighted average values of α, α', $N_{\rm A}$ and $N_{\rm A_2}$. When $|\Delta N_{\rm A_2}| > 0.5$, sufficient reaction events are performed to bring $\sum \Delta N_{\rm A_2}$ back into the range $[-0.5, 0.5]$. In cases where there are insufficient particles in the cell to perform the required number of reaction events, all of the available particles are consumed, and $\sum \Delta N_{\rm A_2}$ is adjusted according to the number of events actually

performed. The limits of ± 0.5 were selected so that the mean $\sum \Delta N_{A_2}$ in each cell during the simulation would be close to zero.

This macroscopic chemistry method is executed after the collision routine. Consequently, there is no need adjust the particle cross-reference arrays during the collision routine to add new atomic particles created by dissociation events and remove atomic particles for recombination events.

B. Extension to complex gas mixtures

In principle, the macroscopic chemistry method may be extended to a complex gas mixture with many species and many reactions. For example, the commonly used *net* reactions in high temperature air, if ionization and charge exchange reactions are ignored, are the dissociation reactions

$$O_2 \rightleftharpoons O + O, \quad N_2 \rightleftharpoons N + N \quad \text{and} \quad NO \rightleftharpoons N + O,$$

and the exchange reactions

$$N + O_2 \rightleftharpoons NO + O \quad \text{and} \quad N_2 + O \rightleftharpoons NO + N.$$

The change in concentration of each species due to each *net* reaction may be determined by solving an appropriate set of ordinary differential equations. In a manner similar to the symmetrical diatomic dissociating gas considered above, the number of reaction events can then be calculated for each net reaction. Methods used to select reacting particles and distribute energy after reactions may differ for each net reaction.

The decoupled approach to DSMC chemistry modeling was applied to a complex reacting chlorine plasma system by Bartel *et al.*[7] and Bartel.[8] The required number of reaction events for each net reaction was calculated from the macroscopic reaction rate using a simple Euler method.

C. Strong shock in dissociating nitrogen

This section presents results obtained using the macroscopic chemistry method to model the structure of a strong shock in nitrogen. The highest enthalpy flow conditions of Kewley and Hornung,[16] as reported by Bird,[17] were simulated. These flow conditions are shown in Table 1. The unbounded simple harmonic oscillator (SHO) vibration model with characteristic vibrational temperature $\Theta_{\text{vib}} = 3390$ K was used.[15] Note that the downstream equilibrium conditions in Table 1 differ slightly from those of Ref. 17. The forward rate constants k^+ were of the Arrhenius form

$$k^+ = C^+ (kT/\epsilon_a)^{\eta^+} \exp[-\epsilon_a/(kT)], \tag{12}$$

and the equilibrium constant K^* was of the common form

$$K^* = C^* (kT/\epsilon_a)^{\eta^*} \exp[-\epsilon_a/(kT)]. \tag{13}$$

For reactions 1 and 2 in nitrogen, Kewley and Hornung[16] give

$$k_1^+ = 1.97 \times 10^{10} \, (T/\Theta_d)^{-2.5} \exp(-\Theta_d/T) \ \text{m}^3/(\text{kmol}\cdot\text{s}) \tag{14}$$

$$\text{and} \quad k_2^+ = 4.71 \times 10^{8} \, (T/\Theta_d)^{-3.5} \exp(-\Theta_d/T) \ \text{m}^3/(\text{kmol}\cdot\text{s}) \tag{15}$$

respectively, where the characteristic dissociation temperature $\Theta_d = \epsilon_a/k = 113200$ K. Ref. 15 gives

$$K^* = 1.8 \times 10^4 \exp\left(-\Theta_d/T\right) \text{ kmol/m}^3.$$

The overall kinetic temperature T_{kin}, as given by Eq. (A4) in the Appendix, was used to calculate k^+ and K^*. It is important to emphasize that the macroscopic chemistry method is *not* restricted to these forms of k^+ and K^*. *Any* equations could be used, which could be *any* function of the macroscopic flow conditions. Different forms are investigated in §V and §VI.

To determine high temperature VHS parameters for $N_2 + N_2$, $N + N$ and $N_2 + N$ collisions, the empirical expressions for $\bar{\Omega}^{(2,2)}_{\text{AB}}$ given by Gupta *et al.*[18] were used to obtain $\mu_{\text{AB}}(T)$ using Eq. (3). Using $T_r = 1000$ K and $\mu_r = \mu_{\text{AB}}(T_r)$, values of υ were selected such that the power law viscosity $\mu = \mu_r(T/T_r)^{1/2+\upsilon}$ gave good agreement with $\mu_{\text{AB}}(T)$. For 1000 K $\leq T \leq$ 20000 K, the difference between this power law viscosity and μ_{AB} was less than 5%. The resulting VHS parameters are shown in Table 2.

The DSMC shock calculations were performed using a code that can simulate normal shocks in gas mixtures with various DSMC chemistry models. Rotational and vibrational energy exchange was performed using the Borgnakke-Larsen method.[10] Following Haas *et al.*,[19] multiple relaxation events were prohibited. The methodology for selecting relaxing particles was that of Gimelshein *et al.*[20] For simplicity, constant relaxation probabilities of 0.30 and 0.01 for rotation and vibration respectively were used. The code employed the downstream piston boundary condition,[1] and particles entering the simulation domain across the upstream boundary were generated according to the method of Ref. 21. The simulations contained 4000 equally sized cells, each with six subcells. The ratio of cell size to the VHS mean free path ${\lambda_{\text{VHS}}}^1$ in the equilibrium upstream and downstream flows was 0.095 and 0.654 respectively. Final sample sizes were $\sim 10^5$ particles per cell. The code used $\Delta t = 0.6\tau_2$, where τ_2 was the downstream mean free time for VHS molecules.[1] A simple Euler method was used to calculate α', so ΔN_{A_2} was given by Eq. (8). The sampling interval was $7\Delta t$. Ten flow samples were used to calculate the required time averaged flow conditions in each cell. Therefore $\dot{\alpha}$ and ΔN_{A_2} were recalculated only once in every 70 time steps, which is a minimal computational overhead.

The resulting normalized profiles of ρ, α and the various kinetic temperatures within the shock are shown in Fig. 1. The methods used to calculate the kinetic temperatures T_{tr}, T_{rot}, T_{vib} and T_{kin} are given in the Appendix. Fig. 1 also includes profiles obtained using a conventional DSMC chemistry method, as discussed in §IV. The normalized density $\hat{\rho}$ is given by

$$\hat{\rho} \equiv \left(\rho - \rho_1\right) / \left(\rho^* - \rho_1\right),$$

and likewise for $\hat{T}_{\text{tr}}$, $\hat{T}_{\text{rot}}$, $\hat{T}_{\text{vib}}$, $\hat{T}_{\text{kin}}$ and $\hat{\alpha}$. The origin of the x-axis has been set to the point at which $\rho/\rho_1 = \rho_2/\rho_1 = 5.93$, which corresponds to $\hat{\rho} = 0.359$. The x-coordinate has been normalized using the nominal mean free path in the upstream gas, given by

$$\lambda_1 = 2\mu_1 / \left(\rho_1 \bar{c}_1\right)$$

where $\bar{c}_1 = \left[8kT_1/(\pi m_{\text{N}_2})\right]^{\frac{1}{2}}$. From Cole and Wakeham,[22] the upstream nitrogen viscosity at $T_1 = 300$ K is $\mu_1 = 17.90$ μPa$\cdot$s, giving $\lambda_1 = 1.0052 \times 10^{-5}$ m. Note that this

real viscosity is higher than the power law viscosity of 15.46 μPa$\cdot$s obtained using the data in Table 2. The difference arises because the VHS parameters in Table 2 were selected to match the real nitrogen viscosity at high temperature. The extent of the simulation domain was approximately $266\lambda_1$.

Downstream profiles of $\hat{\rho}$, $\hat{\alpha}$ and $\hat{T}_{\rm kin}$ are shown in Fig. 2. For computational efficiency, the simulation domain was truncated where the results from the macroscopic method were within $\sim$1% of the equilibrium conditions. For clarity, a 51-point moving average filter was used to smooth the profiles, with a reduced number of points near the downstream boundary.

Experimental values of ρ/ρ_1 downstream of the shock were obtained by Kewley and Hornung,[16] as reported by Bird.[17] These values have been presented in Fig. 3 with the density profiles from Figs. 1 and 2. A first approximation of the errors in the experimental results has been obtained as follows. Firstly, from Ref. 16, the error in the number of fringe shifts F is approximately ± 0.1. By comparing ρ/ρ_1 versus x/λ_1, as given by Ref. 17 with F versus x/λ_1 from Ref. 16, it can be shown that

$$\rho - \rho_1 \approx 0.047F$$

for the flow under consideration. Therefore, the error bounds of ρ/ρ_1 are approximately

$$\frac{\rho \pm 0.1 \times 0.047}{\rho_1} = \rho/\rho_1 \pm 0.63.$$

Secondly, for the 7.31 km/s condition, the mean error in x/λ_1 is approximately ± 8. These approximate error bounds have been included in Fig. 3, and show that the DSMC solution obtained using the macroscopic chemistry method gives acceptable agreement with the experimental results.

D. Rarefied dissociating nitrogen flow over a blunt cylinder

In this section, the rarefied hypersonic flow of dissociating nitrogen over a blunt circular cylinder is considered. An axisymmetric DSMC code was used, with the simulation geometry illustrated in Fig. 4. The code used cell based weighting factors, without subcells. The freestream conditions were $u_\infty = 10^4$ m/s, $\rho_\infty = 1.84 \times 10^{-6}$ kg/m^3 and $T_\infty = 195$ K, which approximate superorbital entry conditions at an altitude of 95 km. These freestream conditions give a frozen Mach number M of 35.1 and $\lambda_{\rm VHS} = 2.563 \times 10^{-2}$ m. The cylinder radius r_c was 0.5 m, with a hot wall at $T_{\rm wall} = 1000$ K with diffuse reflection and full thermal accommodation. The Knudsen number Kn ≈ 0.026 and continuum breakdown parameter $\sim {\rm Kn}M \approx 0.9$ both show that the flow was rarefied,[23] and that large departures from equilibrium conditions are expected. The VHS gas model, reaction rates and equilibrium constant were the same as those used in §IIIC.

The flowfield was computed without chemistry, and also with the macroscopic chemistry method. The initial number of particles N_0 in these calculations was 4×10^5. Steady state was assumed to have been attained after 25 transits of the simulation domain by u_∞. This was confirmed by checking that the number of particles of each species had reach a constant value, within statistical scatter.

The stagnation streamline is approximated by the row of cells adjacent to the flow axis. The resulting normalized profiles of ρ, $T_{\rm tr}$, $T_{\rm rot}$, $T_{\rm vib}$, $T_{\rm kin}$ and α along this stagnation streamline are shown in Figs. 5 to 10. The density profile in Fig. 5 shows a continuous compression up to the cylinder face, which is characteristic of rarefied flows with Kn $\gtrsim 0.01$.[24] Fig. 11 shows profiles of the radial, circumferential and axial translational temperatures, denoted T_r, T_θ and T_z respectively. These profiles, together with the kinetic temperature profiles in Figs. 6 to 8 demonstrate that there was considerable thermal non-equilibrium within the flowfield.

Momentum fluxes and heat fluxes Q to the cylinder face were recorded during each simulation, and the resulting drag coefficients C_D and heat transfer coefficients $C_H = 2Q/(\rho_\infty u_\infty^3)$ are shown in Table 3. The mean total number of particles in each simulation at steady state, denoted $\bar{N}_s$ is also included in Table 3. As expected, chemistry has a negligible effect on C_D, but decreases C_H significantly.

The effects of having few particles in each cell were examined by reducing N_0 to 10^5. The total number of flowfield samples was then increased to obtain a final sample size similar to that for the original case. The resulting profiles are also included in Figs. 5 to 10, and indicate that the number particles per cell has a small effect on the flowfield. For these simulations, $\bar{N}_s$, C_D and C_H are included in Table 3.

This blunt cylinder problem is computationally demanding for the DSMC method due to the high densities and hence small cell sizes required near the cylinder face. The ratio of the cell dimensions in the r and z directions, denoted Δr and Δz respectively, to the local $\lambda_{\rm VHS}$ calculated using $T_{\rm tr}$ was determined. For all cases, $\Delta z/\lambda_{\rm VHS} > 0.5$ and $\Delta r/\lambda_{\rm VHS} > 0.5$ only in a small zone within $\sim 0.06 r_c$ of the face. Also, in a smaller zone within $\sim 0.02 r_c$ of the face, the ratio $\Delta t/\tau_{\rm VHS} > 0.5$, where $\tau_{\rm VHS}$ is the VHS mean collision time[1] calculated using $T_{\rm tr}$. The effects introduced by these inaccuracies will be limited to the small zone near the cylinder face.

IV. COMPARISON WITH A CONVENTIONAL CHEMISTRY METHOD

The above results were compared to those obtained using a conventional DSMC chemistry method. Dissociation reactions were modeled using the method introduced by Bird[25] for bimolecular reactions, which have the general form

$$\mathrm{A} + \mathrm{B} \rightarrow \text{products}.$$

The method assumes that reaction probability, denoted P_R^+ to indicate the forward direction, depends only on the total collision energy ϵ_c, with no biasing towards any particular energy mode, and is therefore referred to as the total collision energy (TCE) method.[26] It is the most common chemistry method used in DSMC calculations.[3,4] The TCE method attempts to recover the Arrhenius rate of Eq. (12) at thermal equilibrium. In the TCE method, the reaction probability P_R^+ is calculated for each collision where ϵ_c exceeds the activation energy ϵ_a. The form of P_R^+ is[25]

$$P_R^+ = \beta \left(1 - \epsilon_a/\epsilon_c\right)^{\chi_1} \left(\epsilon_c/\epsilon_a - 1\right)^{\chi_2}$$

for $\epsilon_c > \epsilon_a$ and zero for $\epsilon_c \leq \epsilon_a$. For mathematical tractability,

$$\chi_1 = \bar{\zeta} + 1 - \upsilon$$

is used, where

$$\bar{\zeta} = \left(\zeta_{\mathrm{rot,A}} + \zeta_{\mathrm{vib,A}} + \zeta_{\mathrm{rot,B}} + \zeta_{\mathrm{vib,B}}\right)/2. \tag{16}$$

Bird[25] gives the method for finding expressions for β and χ_2. Using the g_r and σ_r expressions of Eqs. (1) and (2), these non-dimensional parameters are

$$\beta = \frac{C^+ f_s}{\mathcal{N}\Xi}\left(\frac{T_r}{\Theta_d}\right)^{\frac{1}{2}-\upsilon}\frac{\Gamma(\chi_1+1)}{\Gamma(\chi_1+\chi_2+1)} \quad \text{and} \quad \chi_2 = \eta^+ - \frac{1}{2} + \upsilon,$$

where C^+ and η^+ are the forward rate parameters for the bimolecular reaction, f_s is a symmetry factor that is two for like particles and unity otherwise and $\mathcal{N} = 6.022 \times 10^{26}$/kmol is Avogadro's number. Ξ is a convenient constant with units of m^3/s given by

$$\Xi \equiv \frac{15}{2}\frac{1}{(2-\upsilon)(3-\upsilon)}\frac{kT_r}{\mu_r},$$

which includes the VHS parameters T_r, μ_r and υ of the collision pair.

Eq. (16) shows that $\bar{\zeta}$ depends on ζ_{vib} of each particle participating in the collision. In a DSMC simulation, the effective number of vibrational degrees of freedom ζ_{vib} can be assumed to be a constant value characteristic of the flowfield temperature.[27] Alternatively, using Eqs. (A2) and (A3), $\bar{\zeta}$ can be calculated for each cell using the local vibrational kinetic temperature T_{vib}, which is calculated using a time-weighted average value of ϵ_{vib}. This alternative method has been used here.

Recombination reactions are often ignored in DSMC calculations of reacting flow, because they are relatively infrequent in the low density flows usually simulated. However, in normal shock simulations, recombination reactions must be modeled to achieve an equilibrium state downstream of the shock. Recombination reactions are termolecular, described by

$$\mathrm{A} + \mathrm{B} + \mathrm{M} \rightarrow \mathrm{AB} + \mathrm{M},$$

where M is a third body. Since the DSMC method considers only binary collisions, methods for modeling such reactions cannot use the TCE method as formulated for bimolecular reactions. Here, the DSMC recombination model of Boyd[28] has been used. The recombination probability has the form

$$P_R^- = \left(n_{\mathrm{M}}/n_r\right)\left(\epsilon_c/\epsilon_a\right)^{\kappa},$$

where n_{M} is the time-weighted average third body number density. This probability is applied when collisions occur between atomic particles. The form of P_R^- was selected for mathematical tractability. In a symmetrical diatomic gas,

$$n_{\mathrm{M}} = \rho(1+\alpha)/\left(2m_{\mathrm{A}}\right).$$

Because P_R^- depends on ϵ_c, this recombination method may be regarded as an extension to the TCE method to account for termolecular reactions. The procedure for calculating the parameters n_r and κ is given by Boyd,[28] and the results are

$$\frac{1}{n_r} = \frac{C^+}{C^*}\frac{2}{\mathcal{N}^2\,\Xi}\left(\frac{T_r}{\Theta_d}\right)^{\frac{1}{2}-\upsilon}\frac{\Gamma(7/2+\zeta/2-\upsilon)}{\Gamma(7/2+\zeta/2-\upsilon+\kappa)} \quad \text{and} \quad \kappa = \eta^+ - \eta^* - \frac{1}{2} + \upsilon. \tag{17}$$

Note that C^+ and η^+ apply to the forward dissociation reaction for the recombination reaction being considered, and that the VHS parameters Ξ, T_r and υ refer to collisions between atomic particles. This recombination model is limited in that k^+ and K^* must be in the form of Eqs. (12) and (13) respectively. In Eq. (17), ζ is the mean number of degrees of freedom in the third body. For atomic particles, $\zeta = 0$ and for diatomic particles, $\zeta = 2 + \zeta_{\text{vib}}$, where ζ_{vib} is calculated from the mean cell vibrational temperature.

For the flow conditions in Table 1, shock profiles were computed using the TCE chemistry method, and are shown in Figs. 1 to 3. The simulation conditions were the same as those in §IIIC. It is clear that the results obtained using the macroscopic method are generally in excellent agreement with those obtained using the conventional TCE chemistry method, even within the shock where there is significant thermal non-equilibrium.

For the TCE results, downstream profiles of $\hat{\rho}$, $\hat{\alpha}$ and $\hat{T}_{\text{kin}}$ are shown in Fig. 2. For clarity, smoothing was applied as described in §IIIC, and only one in about 48 points are shown. Fig. 2 shows that the TCE method does not recover the calculated downstream equilibrium conditions. This is because the TCE method gives rates that can differ significantly from the expected Arrhenius rates. These differences arise because the TCE parameters β, χ_2, n_r and κ are derived by assuming that all molecular energy modes are distributed according to continuous distributions, whereas, in common with the code used here, most DSMC codes employ quantum vibration models. Consequently, the actual collision energy distributions occurring in the simulations differ from the assumed continuous distributions, and the rates differ slightly from the expected Arrhenius rates. Gimelshein *et al.*[29] examined this issue for bimolecular reactions, and proposed procedures to account for the use of discrete distributions and recover the Arrhenius rates at equilibrium.

A further effect contributing to the different equilibrium state observed for the TCE method arises because the recombination probability P_R^- can greatly exceed unity where n_{M} is high and ϵ_c is low. In such cases, a single recombination event is performed, resulting in a recombination rate lower than that expected from the Arrhenius rates. This introduces a number density dependence into the recombination rate achieved using the TCE method.

Using the TCE method, the flowfield for the blunt cylinder discussed in §IIID was calculated. Stagnation streamline profiles are included in Figs. 5 to 10, and C_D and C_H are shown in Table 3. There is excellent agreement between the macroscopic and TCE results along the stagnation streamline. The effects of having few particles per cell were also examined for the TCE method, and were found to be negligible.

For the shock simulation results compared in Figs. 1 to 3, the execution time on a single processor for the macroscopic method was 85.5% of that required for the conventional TCE method. The relative CPU times shown in Table 3 also indicate that the macroscopic method is slightly more efficient than the TCE method. It is important to note that the codes used here have not been optimized extensively, and that some improvements in computational efficiency may be possible for both the macroscopic and TCE methods. Some of the improvement in computational efficiency for the macroscopic method can be attributed to the fact that no reactions are computed in equilibrium regions where $\dot{\alpha} = 0$.

V. MACROSCOPIC CHEMISTRY METHOD WITH A DIFFERENT FORM OF RATE EQUATION

The macroscopic chemistry method is not limited to the use of the Arrhenius equation for the forward rate k^+. Other forms of k^+ can be used, and these may be *any* empirical or theoretical function of the macroscopic flow conditions. For example, the two-temperature rate model of Park,[30] which is employed in continuum studies to account for vibrational favoring effects in dissociation reactions, can be used for k^+ in reactions 1 and 2. In this model, a geometrically averaged temperature T_a, given by

$$T_a = T_{\text{tr+rot}}^{s} T_{\text{vib}}^{1-s},$$

is calculated, where $T_{\text{tr+rot}}$ is the kinetic temperature of translation and rotation. For a symmetrical diatomic gas, $T_{\text{tr+rot}}$ is given by Eq. (A4) with $\langle \epsilon_{\text{vib}} \rangle = 0$ and $\zeta_{\text{vib}} = 0$. The average temperature T_a replaces the thermodynamic temperature T in Eq. (12) to give the two-temperature rate k_a^+. For reactions 1 and 2 in nitrogen, Park[30] gives

$$k_{a,1}^+ = 2.46 \times 10^{11} \, (T_a/\Theta_d)^{-1.6} \exp\left(-\Theta_d/T_a\right) \ \text{m}^3/(\text{kmol·s}) \qquad (18)$$

$$\text{and} \quad k_{a,2}^+ = 5.74 \times 10^{10} \, (T_a/\Theta_d)^{-1.6} \exp\left(-\Theta_d/T_a\right) \ \text{m}^3/(\text{kmol·s}) \qquad (19)$$

respectively. Typically, the constant s ranges from 0.5 to 0.7. Lower values of s correspond to higher degrees of vibrational favoring.

The shock conditions of Table 1 were simulated using the two-temperature rates of Eqs. (18) and (19) with $s = 0.5$. To implement the two-temperature model in the macroscopic chemistry method, the rates $k_{a,1}^+$ and $k_{a,2}^+$ replace k_1^+ and k_2^+ respectively when calculating the dissociation rate in Eq. (6). Following Park,[30] an approximate averaged equilibrium constant $K_a^* = K^*(T_a)$ may be used, which replaces K^* in Eq. (6). The resulting density profile, shown in Fig. 12, gives acceptable agreement with the experimental data of Kewley and Hornung.[16]

Also shown in Fig. 12 is the profile obtained using the rates of Eqs. (18) and (19) with the overall kinetic temperature T_{kin} instead of the averaged temperature T_a. These single temperature rates have the Arrhenius form of Eq. (12) and give a density profile in relatively poor agreement with the experimental data. The discrepancy is because the single temperature rates exclude the effects of vibrational favoring provided by the two-temperature rates, resulting in a high initial dissociation rate. This indicates that the macroscopic chemistry method can successfully incorporate the effects of vibrational favoring in dissociation reactions, by using an appropriate two-temperature rate model.

If expressions for k^- are available rather than K^*, Eq. (6) can be written

$$\dot{\alpha} = \frac{\rho}{\mathcal{M}_{\text{A}}} \left[(1-\alpha) Y^+ - \left(\frac{2\rho\alpha^2}{\mathcal{M}_{\text{A}}} \right) Y^- \right],$$

where

$$Y^{\pm} = \alpha k_1^{\pm} + (1-\alpha) k_2^{\pm}/2.$$

Therefore, calculation of $\dot{\alpha}$ does not rely on an expression for the equilibrium constant.

VI. MACROSCOPIC CHEMISTRY METHOD WITH A DIFFERENT FORM OF EQUILIBRIUM CONSTANT

The macroscopic chemistry method is not limited to the use of the common form of the equilibrium constant K^* as given by Eq. (13). Other forms of K^* could be used, and these could be *any* function of the macroscopic flow conditions. Gupta *et al.*[18] gives the equilibrium constant $K^*_{\rm G}$ in the form

$$\ln\left[K^*_{\rm G}(T,n)\right] = \sum_{i=0}^{5} A_i \left[\ln\left(10^4/T\right)\right]^i \tag{20}$$

where $A_i = A_i(n)$. This adds a total number density n dependence into the equilibrium constant, which contrasts with the common expression of Eq. (13) where K^* depends on T alone. This effect is due to the number density dependence of the electronic partition function of the atomic species.[18,30] Park[30] gives a form of the equilibrium constant similar to $K^*_{\rm G}$, and as noted by Boyd and Gökçen,[31] such complex forms of K^* are not mathematically convenient for use in conventional DSMC chemistry models. Gupta *et al.* give A_i values for $10^{19}/\mathrm{m}^3 \leq n \leq 10^{25}/\mathrm{m}^3$. For a given value of n, the values of A_i in Eq. (20) may be estimated by linear interpolation against $\ln n$.

Fig. 13 illustrates the effect of n on the equilibrium constant. The difference between K^* and $K^*_{\rm G}$ is most significant at high temperature and low density, which are the conditions of interest in high enthalpy rarefied gas dynamics. Because the equilibrium constant effectively controls the recombination rate, and because the recombination rate is low, the effects due to different forms of the equilibrium constant in such flows will be small.

To demonstrate the effects of $K^*_{\rm G}$ on the structure of a strong shock, a simulation was performed for the conditions in Table 1 using the macroscopic chemistry method with $K^*_{\rm G}$ rather than K^*. The equilibrium downstream conditions differed slightly from those in Table 1 and were $(\rho^*/\rho_1, T^*/T_1, \alpha^*) = (14.43, 26.23, 0.479)$. The resulting profiles are shown in Fig. 14. In this representation, $\hat{T}_{\rm kin}$, $\hat{T}_{\rm vib}$ and $\hat{\alpha}$ are plotted versus $\hat{\rho}$, which accentuates differences between the results where density gradients are high. All results have been normalized using the downstream equilibrium conditions for K^* from Table 1. The results obtained using $K^*_{\rm G}$ are almost identical to those obtained using K^*. It appears that in flows where the chemistry is primarily dissociative, the number density dependence of the equilibrium constant has little effect on the macroscopic flowfield.

Under low temperature, high density conditions where significant recombination is occurring, the number density dependence of the equilibrium constant will have a significant effect on the recombination rate, and will therefore influence the flowfield. Such effects have been assessed by studying the constant volume recombination of pure atomic nitrogen at a density of 0.2 kg/m^3 and initial temperature of 1000 K. Similar conditions may exist in the stagnation region of hypersonic flow over a blunt body with a cold wall. The calculated equilibrium conditions are $T^* = 9164$ K and $\alpha^* = 0.778$ using K^*, and $T^* = 9520$ K and $\alpha^* = 0.768$ using $K^*_{\rm G}$. Initial and equilibrium number densities are $8.60 \times 10^{24}/\mathrm{m}^3$ and approximately $7.6 \times 10^{24}/\mathrm{m}^3$ respectively. Exact solutions of the relaxation behavior of T and α versus time were calculated using a fourth-order Runge-Kutta method with a time step $\sim |2{\times}10^4{\times}\dot{\alpha}|^{-1}$, and the relaxation

profiles are shown in Figs. 15 and 16 respectively. Different forms of the equilibrium constant give markedly different relaxation profiles.

This relaxation case was simulated with the DSMC method, using the macroscopic chemistry method with both K^* and $K^*_{\rm G}$, and the TCE method. The VHS gas model was the same as that used in §IIIC, and the forward reaction rates were those of Eqs. (14) and (15). The results are shown in Figs. 15 and 16, and demonstrate that the macroscopic chemistry method can accurately simulate the relaxation behavior for forms of the equilibrium constant that differ from the common form of Eq. (13). When using $K^*_{\rm G}$ in the macroscopic chemistry method, a Runge-Kutta method was required to estimate α' for the first time step. For the simulations performed using the TCE method, the relaxation profiles and equilibrium conditions deviate significantly from the expected behavior. This deviation is a result of the difference between the Arrhenius rates and the actual rates given by the TCE method, as discussed in §IV.

VII. DISCUSSION

The macroscopic chemistry method offers significant advantages over conventional DSMC chemistry methods, which are usually limited to assuming the VHS collision model, a particular form of P_R that attempts to reproduce the Arrhenius rates at thermal equilibrium, and a particular form of the equilibrium constant. The macroscopic method can employ reaction rates and an equilibrium constant that are *any* function of the local flow conditions. Furthermore, the macroscopic method allows simple chemistry modeling with any collision model, including realistic potentials such as the Lennard-Jones potential, for which there currently appears to be no means of modeling chemistry in the DSMC method.

The macroscopic chemistry method may offer advantages over conventional DSMC chemistry methods in hybrid codes that employ both continuum solvers and the DSMC method. When using conventional DSMC chemistry methods, such hybrid codes are usually limited to the Arrhenius rate models and the common form of the equilibrium constant. As the macroscopic chemistry method can use any forms of these, this limitation is removed.

In this study, those diatomic particles with higher internal energies are more likely to undergo dissociation. Although this approximates the physics of the dissociation process, it might be regarded as being quite arbitrary, and is a disadvantage of the macroscopic chemistry method. The chemistry procedures of Refs. 7 and 8 offer a means of implementing the decoupled chemistry approach whilst allowing individual reaction events to be modeled with any desired level of physical detail.

The macroscopic chemistry method differs from the conventional approach to DSMC simulations in that macroscopic information derived from all energy modes in a cell, rather than information from individual collisions as they occur, is used to determine the reaction rate. The use of macroscopic conditions in the DSMC method has been used previously. For example, methods for establishing the simulator collision rate in each cell have always used an estimate of the local macroscopic number density. Bird[1] suggested that the rotational and vibrational relaxation numbers could be taken as functions of the cell temperatures. Boyd and Stark[32] proposed a form of P_R for a conventional DSMC chemistry method that included a reaction rate that was

a function of the local macroscopic cell temperature. Also, methods have been proposed whereby any viscosity law $\mu = \mu(T)$ can be incorporated in the DSMC method by using simple collision models that depend on cell kinetic temperatures.[33,34]

At one level, the justification for these approaches is that they can be shown to work efficiently, suggesting that the fine details of collision processes are relatively unimportant. At another level it can be argued that these methods are safer because they do not rely on the physical details of the microscopic collision processes, which are generally poorly known. They use the available macroscopic near-equilibrium information about reaction rates, rotational and vibrational relaxation rates and viscosity laws, but make no detailed assumptions about how the gas behaves far from equilibrium, or how individual collisions proceed. The same near-equilibrium information is usually used to formulate conventional DSMC collision models, with the hope that the models will behave realistically in non-equilibrium situations. Clearly, it would be good if the models did behave realistically far from equilibrium, but often there is no way of knowing if this is so.

VIII. CONCLUSIONS

The macroscopic chemistry method developed here adopts a decoupled approach to chemistry modeling in which collision and reaction processes are simulated separately. The number of reaction events that must be performed in each cell at each time step is determined from rate equations and an equilibrium constant calculated using macroscopic flow conditions. In the test cases examined, this macroscopic method gives results in agreement with those obtained using the conventional TCE chemistry method, even where considerable thermal non-equilibrium conditions exist. Furthermore, the macroscopic method gives results in agreement with experimental data for the density downstream of a strong shock in nitrogen. The number of particles per computational cell appears to have a minimal effect on the results provided by the macroscopic method.

Any rate equations and equilibrium constant can be used with the macroscopic method, and these may be *any* function of the macroscopic conditions. The use of two-temperature rates showed that the macroscopic method can successfully incorporate the effects of vibrational favoring of the dissociation reactions. When the equilibrium constant includes a number density dependence, the resulting constant volume chemical relaxation behavior is accurately modeled using the macroscopic method. Such number density dependence cannot be modeled using current conventional DSMC chemistry methods. For the flow downstream of a strong shock, it appears that the number density dependence of the equilibrium constant has little effect on the flow conditions. The accuracy and flexibility of the macroscopic chemistry method show that it has significant potential for the modeling of rarefied reacting flow with the DSMC method.

IX. ACKNOWLEDGMENT

The authors acknowledge the valuable comments provided by Dr. Tim Bartel of Sandia National Laboratories, Albuquerque, NM, on a draft version of the manuscript.

Appendix: KINETIC TEMPERATURES

For a particular species with molecular mass m, the mean translational thermal energy of velocity component i, denoted $\langle \epsilon_i \rangle$, for the velocity distribution $f(v_i)$ is

$$\langle \epsilon_i \rangle = \frac{m}{2} \int_{-\infty}^{\infty} (v_i - \bar{v}_i)^2 f(v_i) dv_i. \tag{A1}$$

The integral in Eq. (A1) is the variance of the distribution $f(v_i)$. For a sample of N random variates X, the best estimate of the variance of the parent population is[35]

$$S^2(X) = \frac{1}{N(N-1)} \left[N \sum_{j=1}^{N} X_j^2 - \left(\sum_{j=1}^{N} X_j \right)^2 \right].$$

Therefore, the best estimate of $\langle \epsilon_i \rangle$ using a sample of N particles is

$$\langle \epsilon_i \rangle = m S^2(v_i)/2.$$

For a gas mixture containing $N_{\rm sp}$ species,

$$\langle \epsilon_i \rangle = \left(\sum_{s=1}^{N_{\rm sp}} N_s \langle \epsilon_i \rangle_s \right) \times \left(\sum_{s=1}^{N_{\rm sp}} N_s \right)^{-1},$$

where N_s is the number of particles of species s. The mean translational thermal energy of all species in a gas mixture is

$$\langle \epsilon_{\rm tr} \rangle = \langle \epsilon_x \rangle + \langle \epsilon_y \rangle + \langle \epsilon_z \rangle.$$

For velocity component i, the translational kinetic temperature T_i is given by

$$T_i = 2\langle \epsilon_i \rangle / k$$

and the overall translational kinetic temperature $T_{\rm tr}$ is

$$T_{\rm tr} = (T_x + T_y + T_z)/3.$$

In the usual case where rotation is fully excited, diatomic molecules have two rotational degrees of freedom and the rotational kinetic temperature $T_{\rm rot}$ is given by

$$T_{\rm rot} = \langle \epsilon_{\rm rot} \rangle_{\rm A_2} / k.$$

For the unbounded SHO vibration model, the effective number of vibrational degrees of freedom $\zeta_{\rm vib}$ is

$$\zeta_{\rm vib} = \frac{2\Theta_{\rm vib}/T_{\rm vib}}{\exp\left(\Theta_{\rm vib}/T_{\rm vib}\right) - 1}, \tag{A2}$$

where the vibrational kinetic temperature $T_{\rm vib}$ is given by

$$T_{\rm vib} = \frac{\Theta_{\rm vib}}{\ln\left(k\Theta_{\rm vib}/\langle \epsilon_{\rm vib} \rangle_{\rm A_2} + 1\right)}. \tag{A3}$$

The overall kinetic temperature $T_{\rm kin}$ is given by

$$T_{\rm kin} = \frac{2\langle \epsilon \rangle}{k\langle \zeta \rangle} = \frac{2}{k} \times \frac{\langle \epsilon_{\rm tr} \rangle + \langle \epsilon_{\rm rot} \rangle + \langle \epsilon_{\rm vib} \rangle}{3 + (2 + \zeta_{\rm vib})(1-\alpha)/(1+\alpha)}. \tag{A4}$$

Note that $\langle \epsilon_{\rm rot} \rangle = \left[\sum_{j=1}^{N} (\epsilon_{\rm rot})_j \right] / N$ is the mean rotational energy of all particles. Similarly, $\langle \epsilon_{\rm vib} \rangle$ is the mean vibrational energy of all particles.

References

[1]G. A. Bird, *Molecular gas dynamics and the direct simulation of gas flows*, Clarendon Press, Oxford, 1994.

[2]J. K. Harvey and M. A. Gallis, "Review of code validation studies in high-speed low-density flows", J. Spacecraft Rockets **37**, 8 (2000).

[3]I. J. Wysong, R. A. Dressler, Y. H. Chiu, and I. D. Boyd, "Direct simulation Monte Carlo dissociation model evaluation: Comparison to measured cross sections", J. Thermophys. Heat Transfer **16**, 83 (2002).

[4]I. D. Boyd, "Nonequilibrium chemistry modeling in rarefied hypersonic flows", in *Chemical dynamics in extreme environments*, edited by R. A. Dressler, pages 81–137, World Scientific, Singapore, 2001.

[5]I. D. Boyd, D. Bose, and G. V. Candler, "Monte Carlo modeling of nitric oxide formation based on quasi-classical trajectory calculations", Phys. Fluids **9**, 1162 (1997).

[6]I. D. Boyd, G. V. Candler, and D. A. Levin, "Dissociation modeling in low density hypersonic flows of air", Phys. Fluids **7**, 1757 (1995).

[7]T. J. Bartel, J. E. Johannes, and T. R. Furlani, "Trace chemistry modelling with DSMC in chemically reacting plasmas", in *AIAA Paper 98-2753*, Washington, 1998, AIAA.

[8]T. J. Bartel, "Modelling neutral and plasma chemistry with DSMC", in *Rarefied gas dynamics: Proceedings of the 23rd International Symposium*, edited by A. D. Ketsdever and E. P. Muntz, pages 849–856, New York, 2003, American Institute of Physics.

[9]G. A. Bird, "Perception of numerical methods in rarefied gasdynamics", in *Rarefied gas dynamics: Theoretical and computational techniques. Proceedings of the 16th International Symposium*, edited by E. P. Muntz, D. Weaver, and D. Campbell, volume 118 of *Progress in Astronautics and Aeronautics*, pages 211–226, Washington, 1989, AIAA.

[10]C. Borgnakke and P. S. Larsen, "Statistical collision model for Monte Carlo simulation of polyatomic gas mixture", J. Comp. Phys. **18**, 405 (1975).

[11]A. I. Erofeev and V. A. Perepukhov, "Hypersonic rarefied flow about a flat plate by the direct simulation method", in *Rarefied gas dynamics: Proceedings of the 11th International Symposium*, edited by R. Campargue, pages 417–426, Paris, 1979, Commissariat à l'Energie Atomique.

[12]G. A. Bird, "Monte-Carlo simulation in an engineering context", in *Rarefied gas dynamics: Proceedings of the 12th International Symposium*, edited by S. S. Fisher, volume 74 of *Progress in Astronautics and Aeronautics*, Part I, pages 239–255, New York, 1981, AIAA.

[13]S. Chapman and T. G. Cowling, *The mathematical theory of non-uniform gases*, Cambridge University Press, Cambridge, 3rd edition, 1970.

[14]J. O. Hirschfelder, C. F. Curtiss, and R. B. Bird, *Molecular theory of gases and liquids*, John Wiley & Sons, New York, 1954.

[15]W. G. Vincenti and C. H. Kruger, *Introduction to physical gas dynamics*, John Wiley & Sons, New York, 1965.

[16]D. J. Kewley and H. G. Hornung, "Free-piston shock-tube study of nitrogen dissociation", Chem. Phys. Lett. **25**, 531 (1974).

[17]G. A. Bird, "Direct molecular simulation of a dissociating diatomic gas", J. Comp. Phys. **25**, 353 (1977).

[18]R. N. Gupta, J. M. Yos, R. A. Thompson, and K.-P. Lee, *A review of reaction rates and thermodynamic and transport properties for an 11-species air model for chemical and thermal nonequilibrium calculations to 30 000 K*, NASA, Washington, 1990, NASA reference publication 1232.

[19]B. L. Haas, D. B. Hash, G. A. Bird, F. E. Lumpkin, and H. A. Hassan, "Rates of thermal relaxation in direct simulation Monte Carlo methods", Phys. Fluids **6**, 2191 (1994).

[20]N. E. Gimelshein, S. F. Gimelshein, and D. A. Levin, "Vibrational relaxation rates in the direct simulation Monte Carlo method", Phys. Fluids **14**, 4452 (2002).

[21]C. R. Lilley and M. N. Macrossan, "Methods for implementing the stream boundary condition in DSMC computations", Int. J. Numer. Meth. Fluids **42**, 1363 (2003).

[22]W. A. Cole and W. A. Wakeham, "The viscosity of nitrogen, oxygen and their binary mixtures in the limit of zero density", J. Phys. Chem. Ref. Data **14**, 209 (1985).

[23]M. N. Macrossan, H.-H. Chiu, and D. J. Mee, "A test facility for hypervelocity rarefied flows", in *Rarefied gas dynamics: Proceedings of the 22nd International Symposium*, edited by T. J. Bartel and M. A. Gallis, pages 772–779, New York, 2001, American Institute of Physics.

[24]J. K. Harvey, "Direct simulation Monte Carlo method and comparison with experiment", in *Thermophysical aspects of re-entry flows*, edited by J. N. Moss and C. D. Scott, volume 103 of *Progress in Astronautics and Aeronautics*, pages 25–43, Washington, 1986, AIAA.

[25]G. A. Bird, "Simulation of multi-dimensional and chemically reacting flows", in *Rarefied gas dynamics: Proceedings of the 11th International Symposium*, edited by R. Campargue, volume 1, pages 365–388, Paris, 1979, Commissariat à l'Energie Atomique.

[26]B. L. Haas and I. D. Boyd, "Models for direct Monte Carlo simulation of coupled vibration-dissociation", Phys. Fluids A **5**, 478 (1993).

[27]B. L. Haas, "Models of energy-exchange mechanics applicable to a particle simulation of reactive flow", J. Thermophys. Heat Transfer **6**, 200 (1992).

[28]I. D. Boyd, "Analysis of vibration-dissociation-recombination processes behind strong shock waves of nitrogen", Phys. Fluids A **4**, 178 (1992).

[29]S. F. Gimelshein, N. E. Gimelshein, D. A. Levin, M. S. Ivanov, and G. N. Markelov, "Modeling of rarefied hypersonic flows over spacecraft in Martian atmosphere using the DSMC method", in *AIAA Paper 2002-2759*, Washington, 2002, AIAA.

[30]C. Park, *Nonequilibrium hypersonic aerothermodynamics*, John Wiley & Sons, New York, 1990.

[31]I. D. Boyd and T. Gökçen, "Evaluation of thermochemical models for particle and continuum simulations of hypersonic flow", J. Thermophys. Heat Transfer **7**, 406 (1993).

[32]I. D. Boyd and J. P. W. Stark, "Direct simulation of chemical reactions", J. Thermophys. **4**, 391 (1990).

[33]M. N. Macrossan, "ν-DSMC: A fast simulation method for rarefied flow", J. Comp. Phys. **173**, 600 (2001).

[34]M. N. Macrossan, "μ-DSMC: A general viscosity method for rarefied flow", J. Comp. Phys. **185**, 612 (2003).

[35]R. E. Walpole and R. H. Myers, *Probability and statistics for engineers and scientists*, Macmillan Publishing Company, New York, 4th edition, 1989.

TABLES

ρ_1	=	7.48×10^{-3}	kg/m^3	ρ_2/ρ_1	=	5.93
u_1	=	7.31	km/s	T_2/T_1	=	84.34
T_1	=	300	K	ρ^*/ρ_1	=	14.72
M_1	=	20.71		T^*/T_1	=	25.62
α_1	=	0		α^*	=	0.486

Table 1: Flow conditions of Kewley and Hornung,[16] as reported by Bird.[17] The subscript 1 refers to upstream conditions, the subscript 2 refers to Rankine-Hugoniot conditions downstream of a vibrationally and chemically frozen shock, and the superscript * refers to equilibrium downstream conditions calculated using K^* from Eq. (13).

Collision partners	μ_r (μPa·s)	υ	σ_r (m^2)	g_r (m/s)
$N_2 + N_2$	38.61	0.26	4.991×10^{-19}	1089
$N + N$	44.75	0.28	3.118×10^{-19}	1541
$N_2 + N$	36.87	0.29	4.421×10^{-19}	1334

Table 2: High temperature viscosity and VHS parameters for N_2 and N. In all cases, $T_r = 1000$ K was used.

Chemistry method	$N_0/10^3$	$N_s/10^3$	C_D	C_H	Relative CPU time
No chemistry	400	790.4	1.772	0.288	0.99
Macroscopic	400	870.0	1.772	0.234	1
Macroscopic	100	217.7	1.772	0.232	1.15
TCE	400	868.4	1.772	0.232	1.09
TCE	100	216.9	1.772	0.231	1.23

Table 3: Summary of blunt cylinder simulation results. N_0 refers to the initial number of particles, and $\bar{N}_s$ refers to the mean number of particles during sampling at steady state.

FIGURES

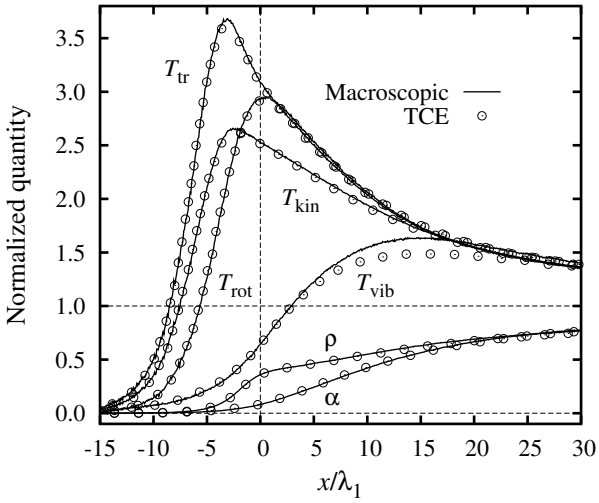

Figure 1: Normalized profiles of ρ, $T_{\rm tr}$, $T_{\rm rot}$, $T_{\rm vib}$, $T_{\rm kin}$ and α within a Mach 20.71 shock in nitrogen, calculated using the macroscopic and conventional TCE chemistry methods.

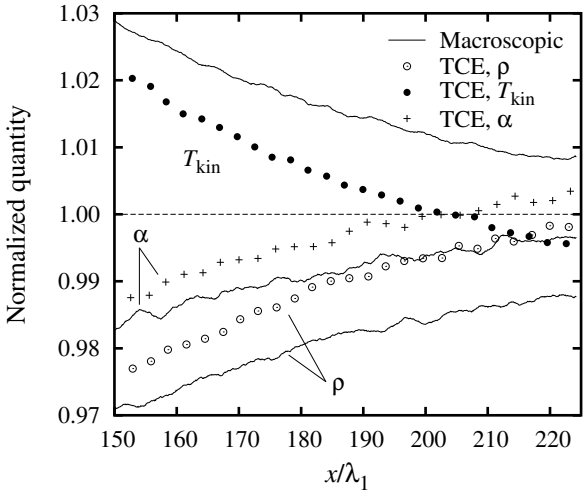

Figure 2: Normalized profiles of ρ, $T_{\rm kin}$ and α downstream of a Mach 20.71 shock in nitrogen. Some smoothing has been applied for clarity, as detailed in §IIIC. The profiles calculated using the macroscopic method approach the calculated equilibrium conditions, whereas those for the conventional TCE method do not.

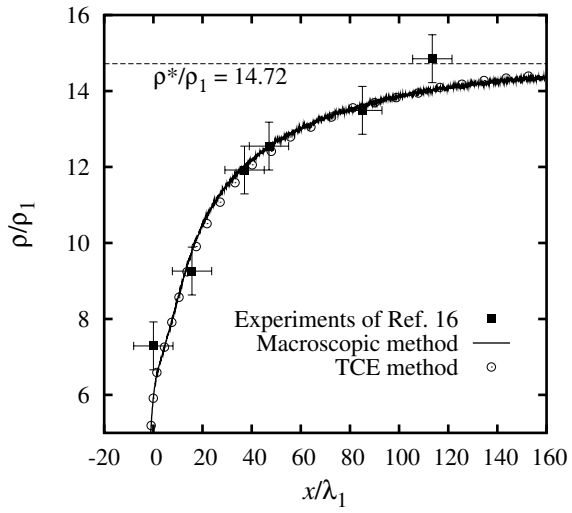

Figure 3: Profiles of density ratio ρ/ρ_1 downstream of a Mach 20.71 shock in nitrogen, calculated using the macroscopic and conventional TCE chemistry methods. Experimental data points of Kewley and Hornung,[16] as reported by Bird,[17] are included, with approximate error bars.

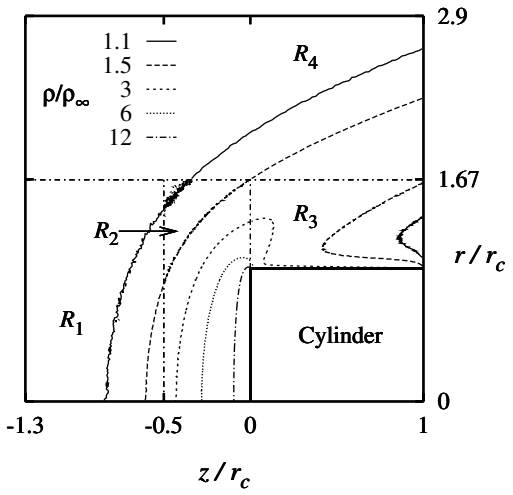

Figure 4: Geometry of simulation domain for blunt cylinder calculations with ρ/ρ_∞ contours. Region i is indicated by R_i. Each region had a regular rectangular grid. In R_1, the numbers of cells in the (z, r) directions were $(100, 150)$. In R_2, R_3 and R_4, the numbers of cells were $(100, 500)$, $(70, 200)$ and $(120, 60)$ respectively.

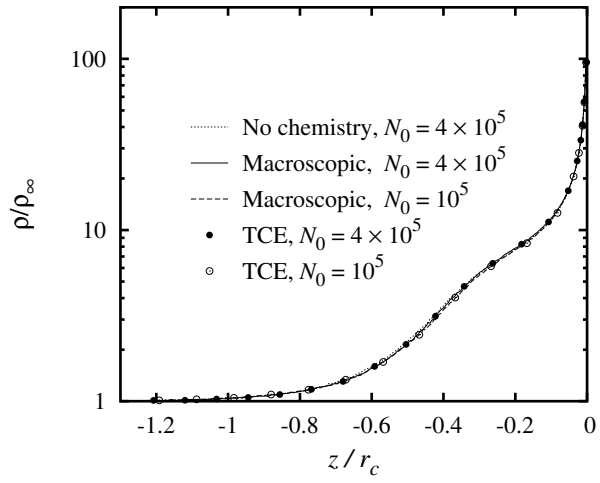

Figure 5: Profiles of ρ/ρ_∞ along the stagnation streamline for the blunt cylinder simulations.

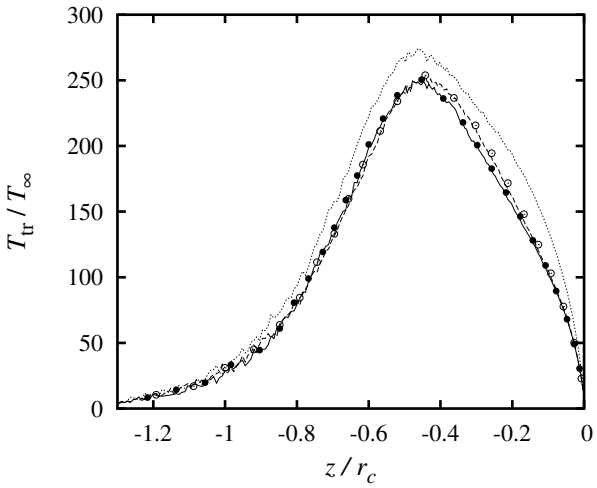

Figure 6: Profiles of $T_{\rm tr}/T_\infty$ along the stagnation streamline for the blunt cylinder simulations. The key is given in Fig. 5.

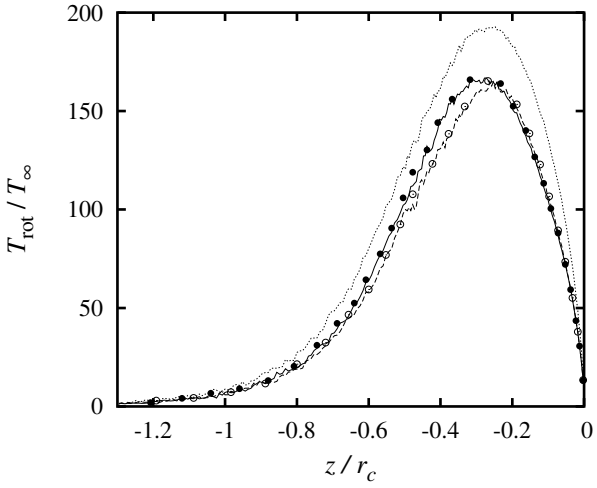

Figure 7: Profiles of $T_{\rm rot}/T_\infty$ along the stagnation streamline for the blunt cylinder simulations. The key is given in Fig. 5.

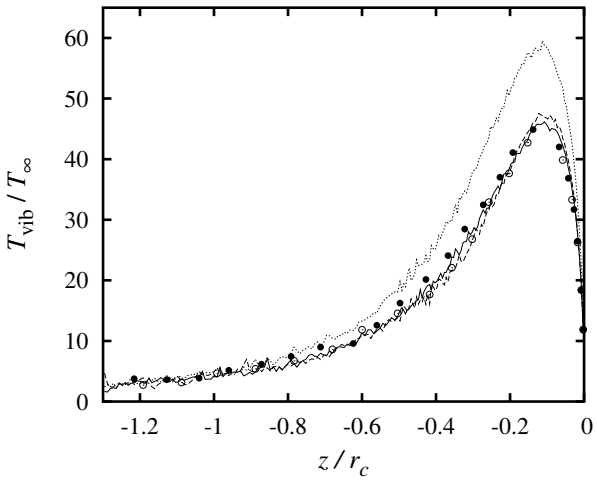

Figure 8: Profiles of $T_{\rm vib}/T_\infty$ along the stagnation streamline for the blunt cylinder simulations. The key is given in Fig. 5.

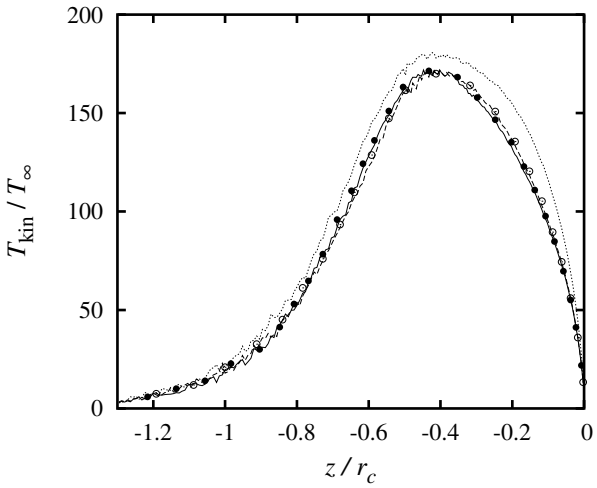

Figure 9: Profiles of $T_{\rm kin}/T_\infty$ along the stagnation streamline for the blunt cylinder simulations. The key is given in Fig. 5.

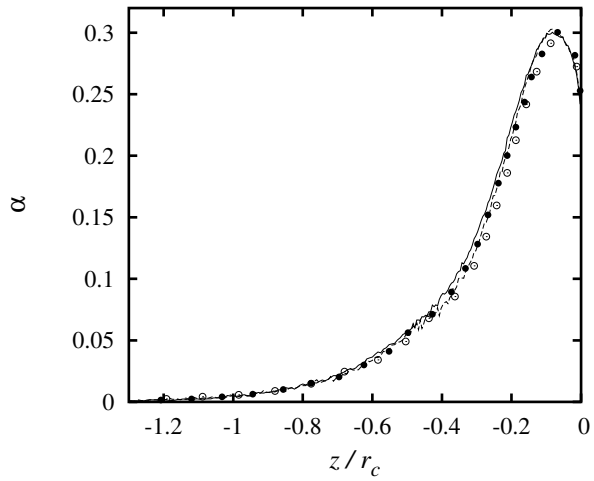

Figure 10: Profiles of α along the stagnation streamline for the blunt cylinder simulations. The key is given in Fig. 5.

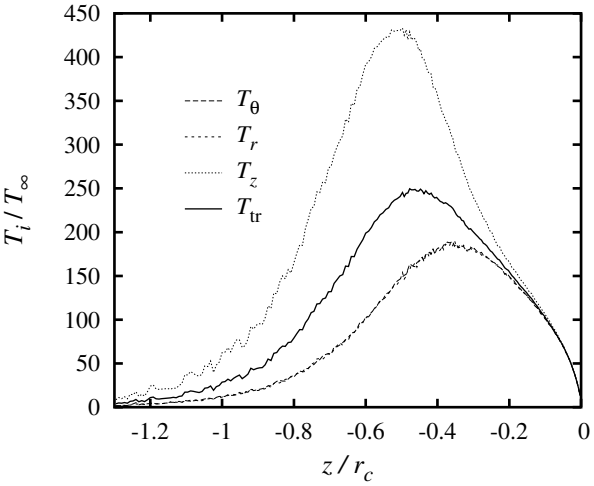

Figure 11: Profiles of translational temperatures along the stagnation streamline for the blunt cylinder simulations using the macroscopic chemistry method with $N_0 = 4 \times 10^5$.

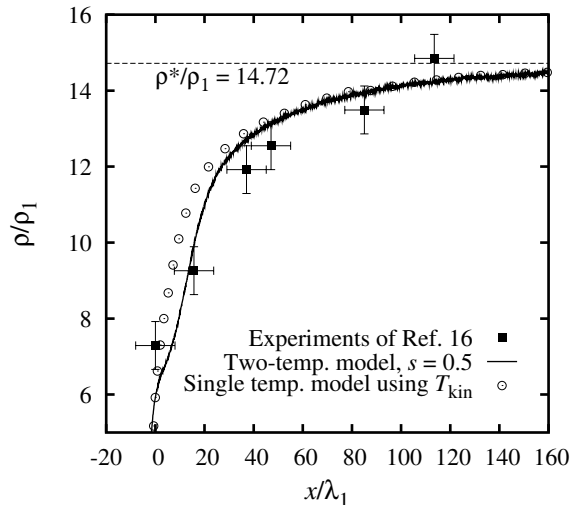

Figure 12: Profile of density ratio ρ/ρ_1 downstream of a Mach 20.71 shock in nitrogen, calculated using the macroscopic chemistry method with the two-temperature rate model of Park.[30] The profile obtained using the single temperature rates with $T_{\rm kin}$, which have the Arrhenius form, instead of the two-temperature model is also shown.

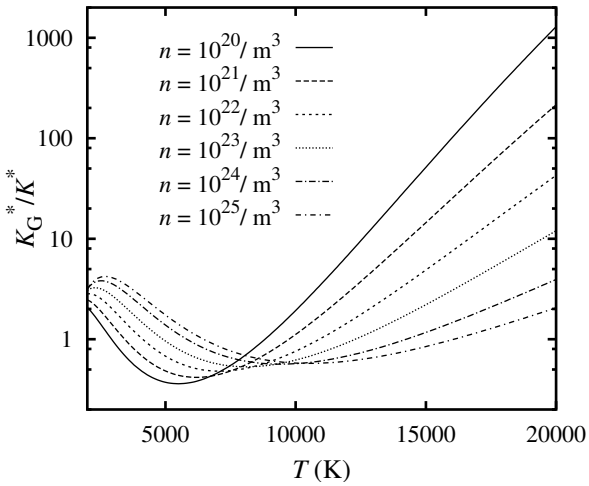

Figure 13: Ratio of the number density dependent equilibrium constant $K^*_{\rm G}$ of Gupta *et al.*[18] to the common form of the equilibrium constant K^*, for dissociating nitrogen.

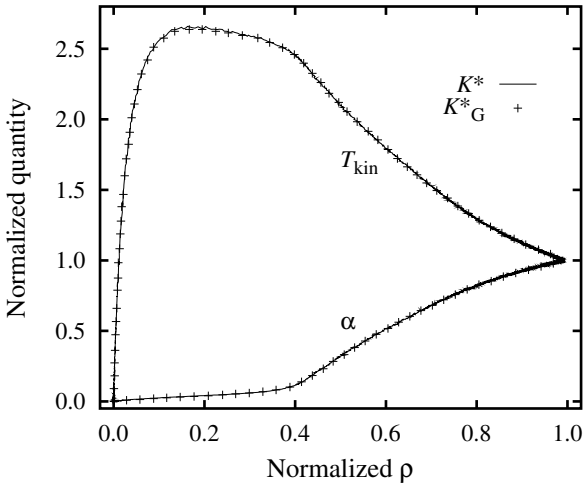

Figure 14: Normalized profiles of T_{kin} and α versus normalized ρ for a Mach 20.71 shock in nitrogen, calculated using the macroscopic chemistry method. Results are shown for calculations using the common form of the equilibrium constant K^* from Eq. (13), and the form given by Gupta *et al*[18] from Eq. (20), denoted K^*_{G}, which includes a number density dependence.

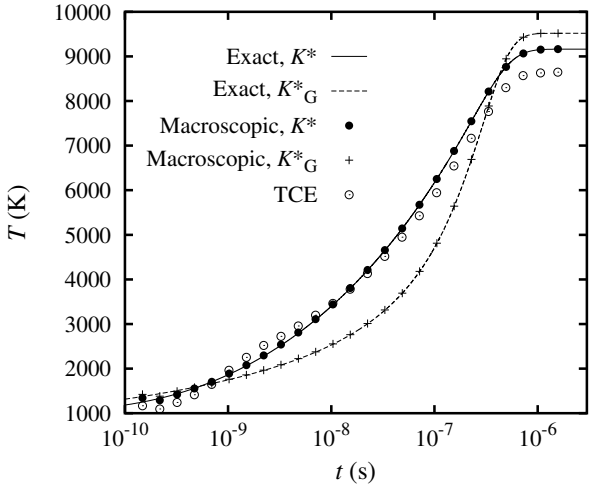

Figure 15: Temperature profiles for constant volume recombination of atomic nitrogen with different forms of the equilibrium constant. "Exact" Runge-Kutta continuum solutions are compared to DSMC solutions obtained using both the macroscopic and TCE chemistry methods.

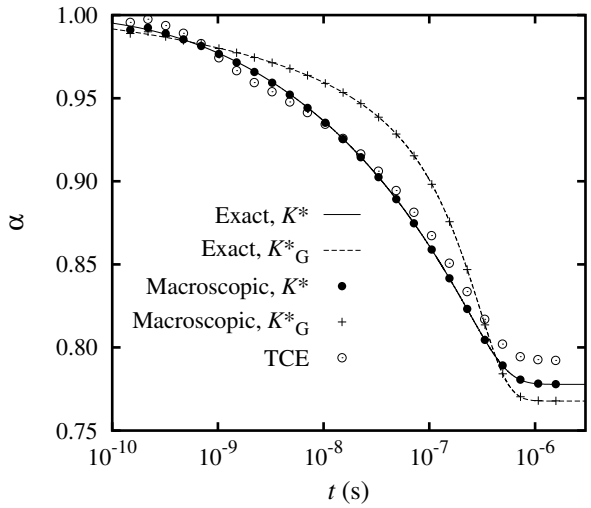

Figure 16: Profiles of dissociation fraction α for the constant volume recombination of atomic nitrogen with different forms of the equilibrium constant. "Exact" Runge-Kutta continuum solutions are compared to DSMC solutions obtained using both the macroscopic and TCE chemistry methods.